

NANO EXPRESS

Open Access



Multicolor Emitting N-Doped Carbon Dots Derived from Ascorbic Acid and Phenylenediamine Precursors

Linlin Wang, Won Mook Choi, Jin Suk Chung and Seung Hyun Hur*

Abstract

In this research, we report the green, blue, and orange color emitting N-doped carbon dots (CDs), which are being synthesized from ascorbic acid and *o*-/*m*-/*p*-phenylenediamine (*o*-PDA, *m*-PDA, and *p*-PDA, respectively). The effects of the solvent polarity and solution pH on the PL emission properties of the as-synthesized CDs have been systematically investigated. It has been observed that the PL emission of the as-synthesized CDs decreases with the increase in solvent polarity due to the greater agglomeration. The surface charge of CDs also shows prominent effects on the pH-dependent PL emission properties.

Keywords: Multicolor emission, N-doped carbon dots, Ascorbic acid, Phenylenediamine, Hydrothermal

Introduction

Recently, fluorescent carbon dots (CDs) have drawn considerable attention owing to their high quantum yields, low toxicity, excellent biocompatibility, and facile preparation procedures [1–4]. CDs can be widely used in sensing, display, and bioimaging applications. Most of CDs emit in blue or green region that limits their application in living tissue imaging since this process needs deep penetration of light and removal of autofluorescence as well as background light scattering related limitations. Henceforth, synthesis of CDs that emit at larger wavelength has become important. In this regard, green chemical synthesis of multi-color emissive CDs is important that would exclude the associated synthetic hazards and critical separation steps [5].

Adjusting the surface of CDs by doping of hetero atoms, such as nitrogen (N), boron (B), and sulfur (S) atoms, can be used to modify the fluorescence properties of CDs. For this purpose, organic/inorganic molecules with hetero-atom functionalities might be used

as co-precursor along with the carbon source or as precursor [6–8]. Phenylenediamine isomers [*o*-phenylenediamine (*o*-PDA), *m*-phenylenediamine (*m*-PDA), and *p*-phenylenediamine (*p*-PDA)], with amine ($-\text{NH}_2$) functionalities, have proved to be efficient heteroatom source for synthesis of N-doped CDs [3, 9, 10].

In this work, the green, blue, and orange color emitting N-doped CDs were successfully synthesized from hydrothermal treatment of ascorbic acid (AA) and individual *m*-PDA, *o*-PDA, and *p*-PDA, respectively (*Am*-, *Ao*-, and *Ap*-CDs, respectively). The effects of the reaction conditions and solvents, and pH of solution on the fluorescence properties of each type of CDs were systematically investigated. In particular, green color emitting CDs synthesized from ascorbic acid and *m*-PDA exhibited very high quantum yield (QY) in the ethanol solvent.

Experimental Methods

Detailed information on the materials and instrumental analysis are described in Additional file 1: Section S1 and S2.

*Correspondence: shhur@ulsan.ac.kr

School of Chemical Engineering, University of Ulsan, Daehak-ro 93, Nam-gu, Ulsan 44610, Republic of Korea

Synthesis of *Am*-, *Ao*-, and *Ap*-CDs

To prepare *Am*-CDs, ascorbic acid (0.1 M, 0.8 mL) and *m*-phenylenediamine (0.1 M, 0.8 mL) (ratio of AA: *m*-PDA = 1:1) were added into 10.4 mL deionized water, and stirred for 5 min. Then, the mixture was transferred into a 50 mL Teflon-lined autoclave, and heated and maintained at 160 °C for 6 h in an oven for further reaction. After cooling down to room temperature (RT), the *Am*-CDs were collected after removing the suspended particles via centrifugation at 10,000 rpm for 20 min, and further purified by dialysis tube for 6 h to remove the residual chemicals. The as-obtained *Am*-CDs solution was stored at 4 °C for further characterization.

To prepare *Ao*-CDs and *Ap*-CDs, all experimental procedures were the same as those of *Am*-CDs, except for the precursor ratio. For *Ao*-CDs, ascorbic acid (0.1 M, 1.2 mL) and *o*-phenylenediamine (0.1 M, 0.8 mL) (ratio of AA: *o*-PDA = 3:2) were used; and for *Ap*-CDs, ascorbic acid (0.1 M, 0.8 mL) and *p*-phenylenediamine (0.1 M, 0.4 mL) (ratio of AA: *p*-PDA = 2:1) were used, respectively.

Additional file 1: Fig. S1 shows that the reaction temperature and the precursor ratio were optimized to obtain the highest fluorescence for each CDs.

Figure 1 shows that the emission intensity and wavelength of the as-synthesized CDs are totally different from those of the precursor materials. The overall comparison is summarized in Additional file 1: Table S1. It is interesting to note that green emitting *Am*-CDs can be obtained from cyan and blue emitting AA and *m*-PDA, while blue color emitting *Ao*-CDs can be obtained from cyan and yellow emitting AA and

o-PDA, which indicates the new conjugated structure formed from the reaction between AA and PDAs.

Quantum Yield Measurement

The quantum yields (QYs) of the *Am*-, *Ao*-, and *Ap*-CDs were obtained by a well-known relative slope method at RT using various dyes that match their emissions with those of each CDs [9]. For *Am*-CDs (excitation wavelength of 450 nm), Rhodamine 101 in ethanol (QY = 100%) was selected as the reference; for *Ao*-CDs (excitation wavelength of 360 nm), quinine sulfate (QS) in 0.1 M sulfuric acid solution (QY = 54%); and for *Ap*-CDs (excitation wavelength of 514 nm), rhodamine B in water (QY = 31%).

To calculate the QYs, the integrated PL intensities of the sample and reference were plotted against absorbance at several concentrations, and the gradients were obtained and compared.

The QYs of the three CDs were obtained from the following equation:

$$\Phi_s = \Phi_r * \frac{K_s}{K_r} * \frac{\eta_s}{\eta_r} \quad (1)$$

where Φ is the relative quantum yield, K is the slope of the fitted line, and η is the refractive index of the solvent. The subscript “r” refers to the reference, and “s” to the sample. The values of refractive index for water and ethanol are 1.33 and 1.36, respectively.

Results and Discussion

Characterization of the As-Synthesized CDs

The morphology and size of the *Ax*-CDs ($x = m, o,$ and p) were analyzed from TEM images. Figures 2, 3, and 4

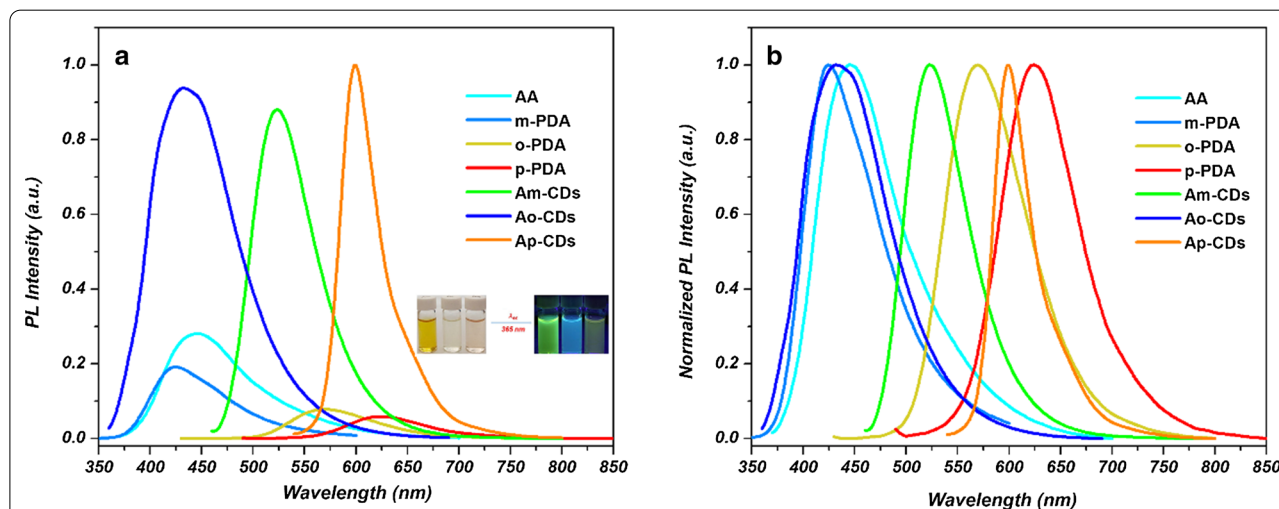


Fig. 1 **a** Fluorescence spectra, and **b** normalized fluorescence spectra of *Ax*-CDs and various precursor materials. Inset: Photographs of *Am*-CDs, *Ao*-CDs, and *Ap*-CDs dispersed in water under natural light (left), and under UV irradiation ($\lambda_{\text{ex}} = 365$ nm) (right)

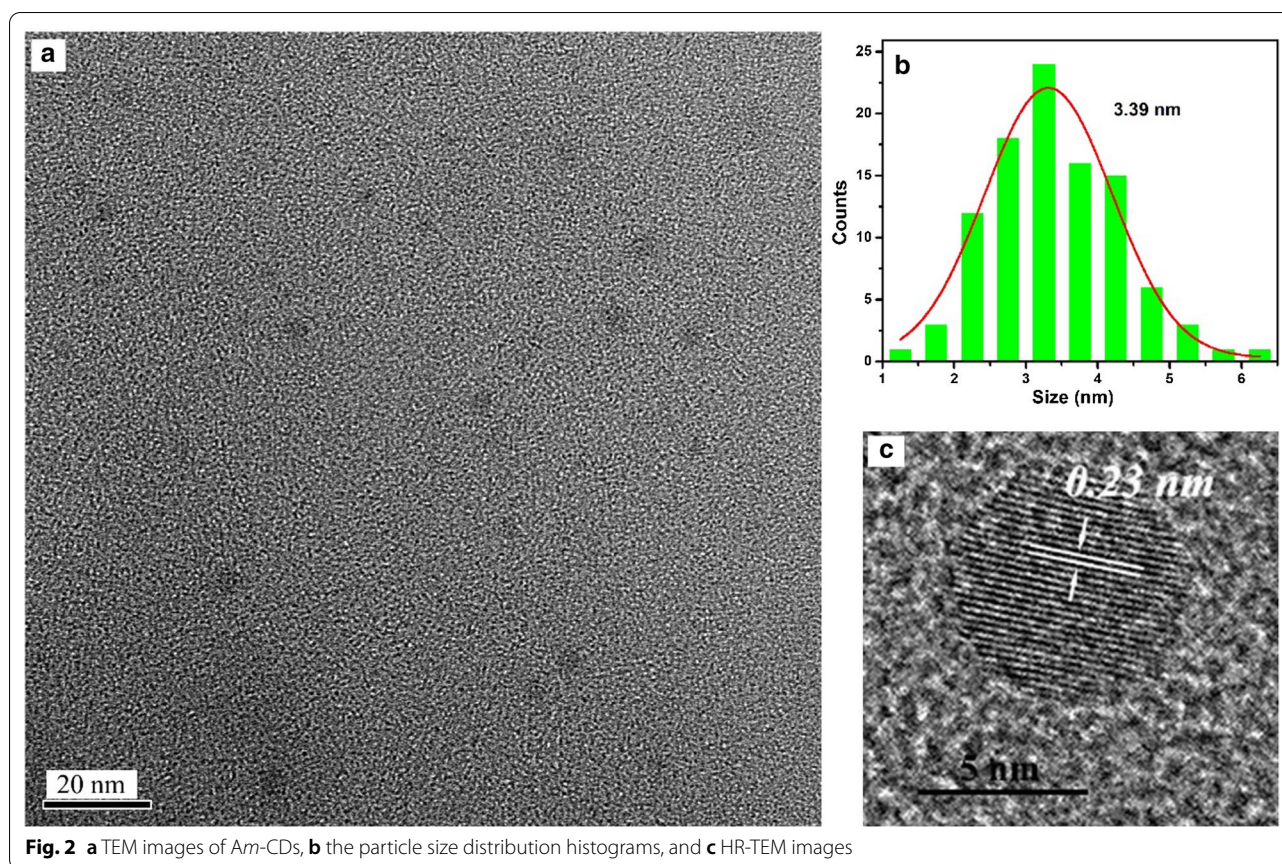


Fig. 2 **a** TEM images of *Am*-CDs, **b** the particle size distribution histograms, and **c** HR-TEM images

show that the mean diameters of *Am*-CDs, *Ao*-CDs, and *Ap*-CDs were 3.39 nm, 3.65 nm, and 4.45 nm, respectively. The interplanar spacings of *Ax*-CDs were 0.23 nm, 0.21 nm, and 0.35 nm analyzed from HR-TEM images, respectively, which correspond to the (100) and (002) planes of graphite carbon [11].

The crystal structures of the *Ax*-CDs were investigated by XRD. Figure 5a shows that the three CDs have a broad single diffraction peak around $2\theta = 21^\circ - 23^\circ$, which originates from graphitic carbon structure [3, 12].

The chemical bonds and surface functional groups of *Ax*-CDs were analyzed by FT-IR spectra. Figure 5b shows the peaks at ~ 3460 and $\sim 3313 - 3353$ cm^{-1} that can be attributed to the stretching vibrations of O–H and N–H, respectively. The presence of hydrophilic groups can improve the solubility of CDs in polar solvent by the formation of hydrogen bonding [13, 14]. The peaks at ~ 1070 , ~ 2877 and ~ 2964 cm^{-1} can be assigned to the stretching vibrations of C–H [8]. The strong peak observed at ~ 1633 cm^{-1} can be ascribed to the stretching vibration of C=O bond in the amide group, which confirms the amidation reaction between the carboxylic acids of AA and amines of PDAs [15]. The peaks that appear at ~ 1520 cm^{-1} can originate from the bending

vibration of C=C [16]. In addition, the peaks observed at ~ 1361 cm^{-1} can be ascribed to the stretching vibration of C–N, which confirms the presence of nitrogen atom in the as-synthesized CDs [10]. The near identity of the FT-IR spectra of all three CDs indicates the presence of similar chemical bonds and functional groups on the CDs, regardless of the position of amine group in PDA isomers species.

XPS was used to analyze the elemental composition and functional groups of the *Ax*-CDs. Figure 6a shows the XPS survey spectrum of *Am*-CDs, which indicates the existence of C, O, and N atoms in the synthesized *Am*-CDs. Additional file 1: Figs. S2 and S3 show that the three CDs have similar elemental compositions, as summarized in Table 1. The XPS analyses also indicate similar oxidation state and functionalities in the three CDs. Figure 6, and Additional file 1: Figs. S2 and S3 show the high-resolution C1s XPS spectra for *Ax*-CDs, which reveal that carbon can be deconvoluted into several peaks centered at ~ 284.0 , ~ 285.2 , ~ 286.9 , and ~ 290.1 eV, which correspond to C=C, C–C, C–O, and N–C=O groups, respectively. The high-resolution O1s spectra can be deconvoluted into peaks shown at ~ 531.8 and ~ 532.8 eV that can be attributed to C=O and C–O groups,

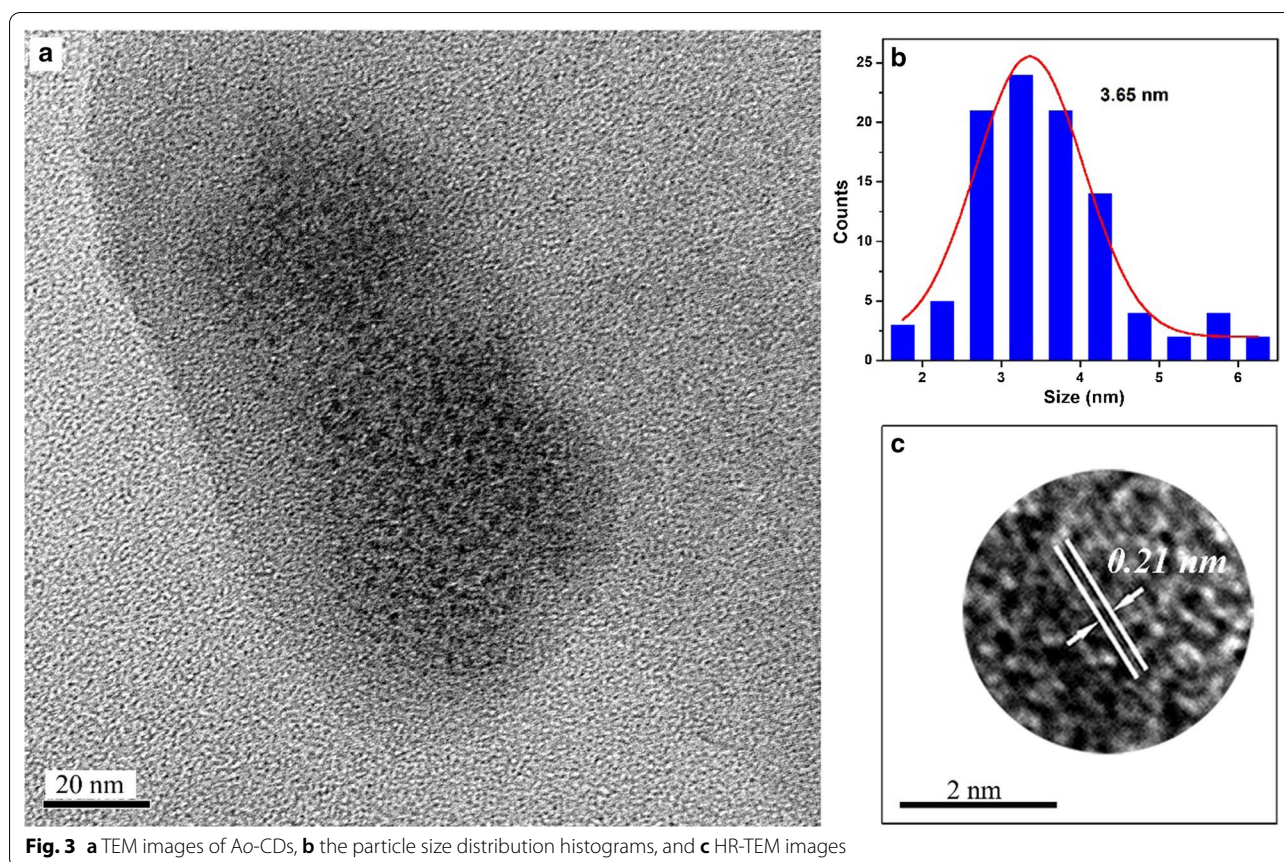


Fig. 3 **a** TEM images of Ao-CDs, **b** the particle size distribution histograms, and **c** HR-TEM images

respectively [17]. The N1s spectra reveal the presence of N–H, C–N–C, and graphitic N groups shown at ~ 399.0 , ~ 400.0 , and ~ 401.4 eV, respectively [18].

Optical Properties of the Ax-CDs

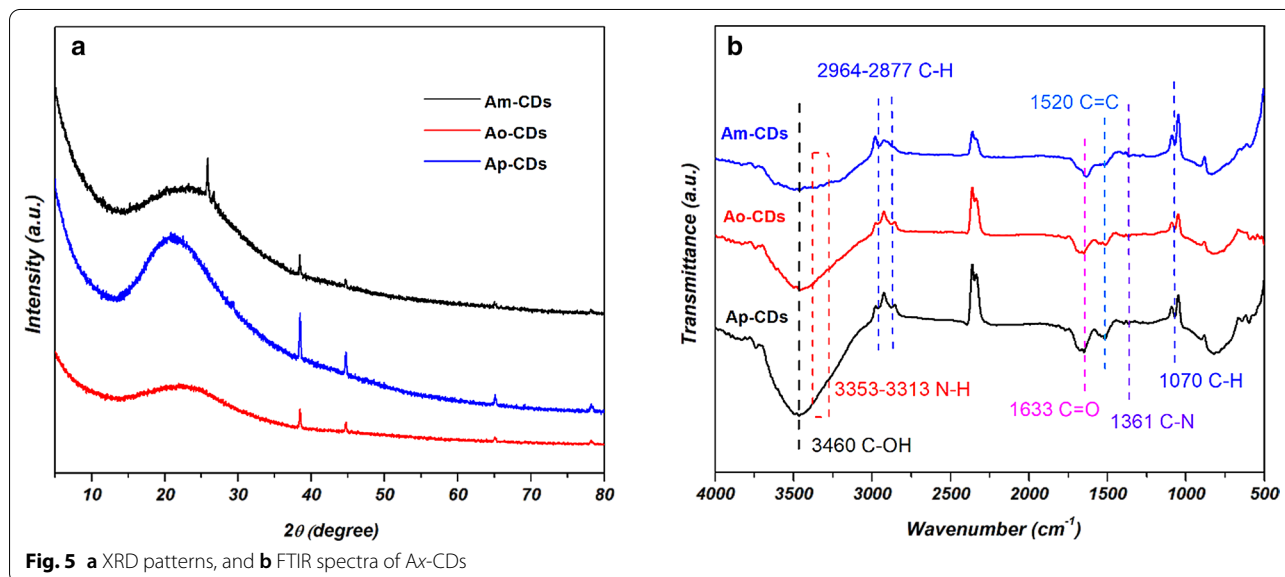
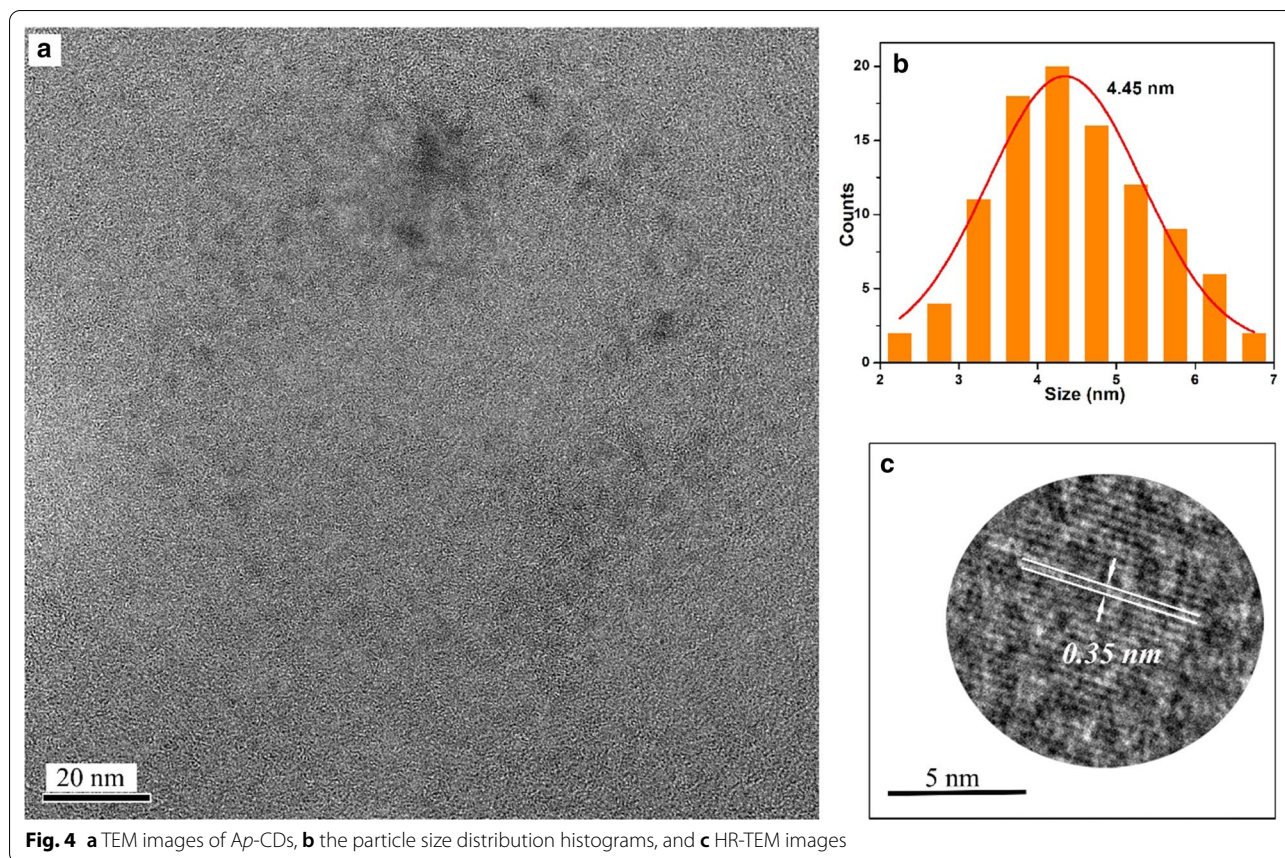
The optical properties of the Ax-CDs were explored by the UV–Vis absorption and PL spectra. Figure 7 shows the UV–Vis absorption, photoluminescence excitation (PLE), and PL spectra of the Ax-CDs. Two absorption peaks centered at 289 and 400 nm are observed in the UV–Vis absorption of Am-CDs (Fig. 7a), which correspond to the π – π^* transitions of the C=C structure, and the n – π^* transitions of C=O groups [15]. Ao-CDs and Ap-CDs showed two peaks in the UV–Vis spectra, however the peak positions and intensities were different (Fig. 7c, e). This difference might be attributed to the different extent of electronic transitions. Moreover, the additional broad absorption peak shown at ~ 510 nm can be attributed to the surface absorption of the Ap-CDs, and succedent excitation of the PL emission [19]. Accordingly, the PLE and PL spectra are different for all three Ax-CDs. The Am-CDs show emission in the green region at 521 nm when excited at 450 nm. The Ao-CDs and Ap-CDs show excitation peaks at 360 and 580 nm

and emit at blue region at 432 nm and orange region at 596 nm, respectively.

Figures 7b, d, f show that Am- and Ao-CDs show excitation-dependent emission while Ap-CDs show excitation-independent emission. The excitation wavelength-dependent PL emission behavior might originate from the nonuniform CDs size, and presence of various surface defects, and various surface functional groups in the CDs [20, 21]. The excitation wavelength-independent PL emission behavior of Ap-CDs indicates uniform emission states, which also result in narrow emission width. The different excitation wavelength related PL properties among the Ax-CDs imply the different energy states, and their morphology [22, 23].

Solvent Effects and QY on the PL Emission Properties

The effects of solvent, including deionized water (H₂O), Methanol (MeOH), Ethanol (EtOH), Isopropyl alcohol (IPA), Acetone (ACE), Acetonitrile (ACN), *N,N*-Dimethylformamide (DMF), and Dimethyl sulfoxide (DMSO) on the PL emission properties of the Ax-CDs were investigated. Additional file 1: Fig. S4 shows that the PL emission wavelength changes at different solvents. This shows the typical solvatochromic properties of CDs caused by



the interaction between surface functional groups of CDs and solvents [21, 24].

Additional file 1: Fig. S5 shows that the *Am*-CDs possessed the highest QY among the three CDs. In addition,

the *Ax*-CDs in ethanol solvent exhibit higher QY than those in water, which can be explained by (1) higher extent of agglomeration of CDs in high polar solvent, (2) increased rate of non-radiative decay during the

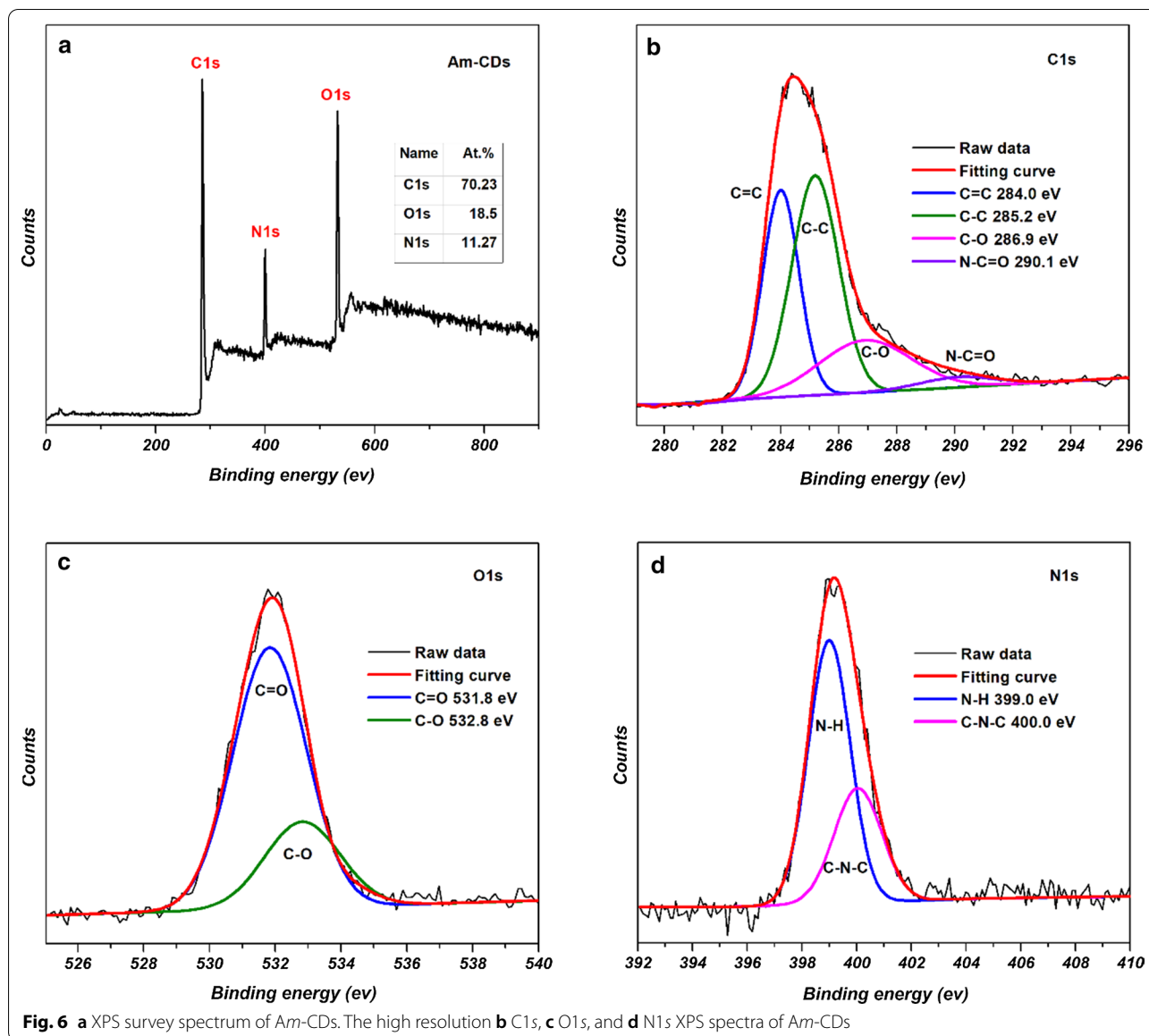


Table 1 The elemental compositions of Ax-CDs

Sample	C (%)	O (%)	N (%)
Am-CDs	70.23	18.50	11.27
Ao-CDs	69.30	21.85	8.85
Ap-CDs	70.63	20.28	9.09

interaction between highly polar solvent and CDs, and (3) water-induced morphological change [25].

pH Effects on the Fluorescence Emission of Ax-CDs

The PL emission intensities of the as-prepared Am-, Ao-, and Ap-CDs were monitored at various pH

conditions. Figure 8 shows that Am- and Ao-CDs exhibit similar PL emission behavior as the pH of solution changes. The decrease in PL emission as the pH increases can be attributed to the deprotonation of the surface functional groups of the Am- and Ao-CDs, resulting in the agglomeration of CDs [26–29].

On the other hand, for Ap-CDs, the PL intensity increases as the pH of solution increases. This phenomenon can be attributed to the different surface charge of Ap-CDs from the other CDs.

To investigate the different pH-dependent behaviors between Ax-CDs, the zeta potential was monitored at various pH values. As shown in Fig. 9, the zeta potentials of the Am- and Ao-CDs gradually decreased with

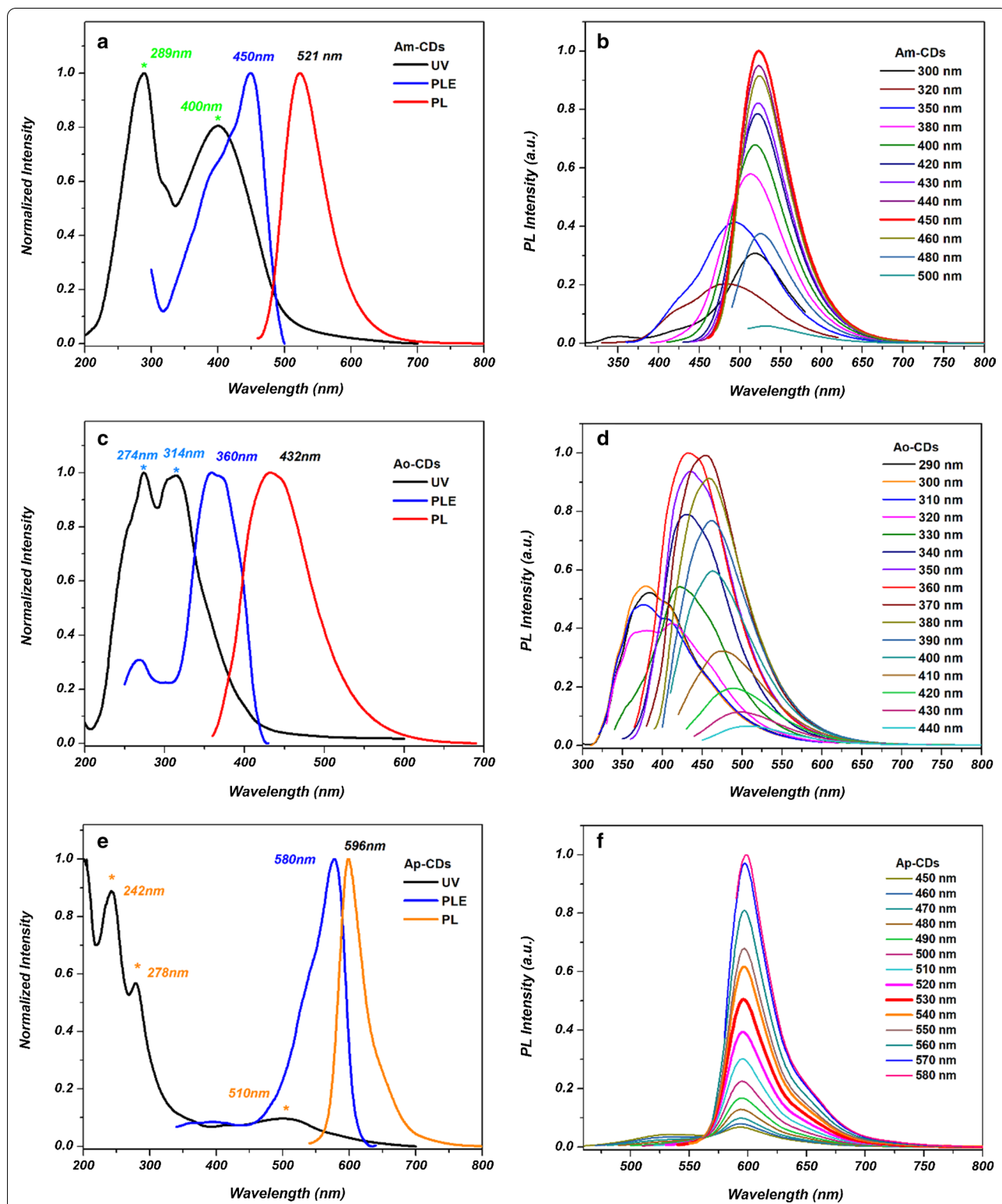


Fig. 7 The normalized UV-Vis absorption spectra, PL excitation, and PL emission spectra of the **a** Am-CDs, **c** Ao-CDs, and **e** Ap-CDs. The normalized PL emission spectra of the **b** Am-CDs, **d** Ao-CDs, and **f** Ap-CDs at different excitation wavelengths

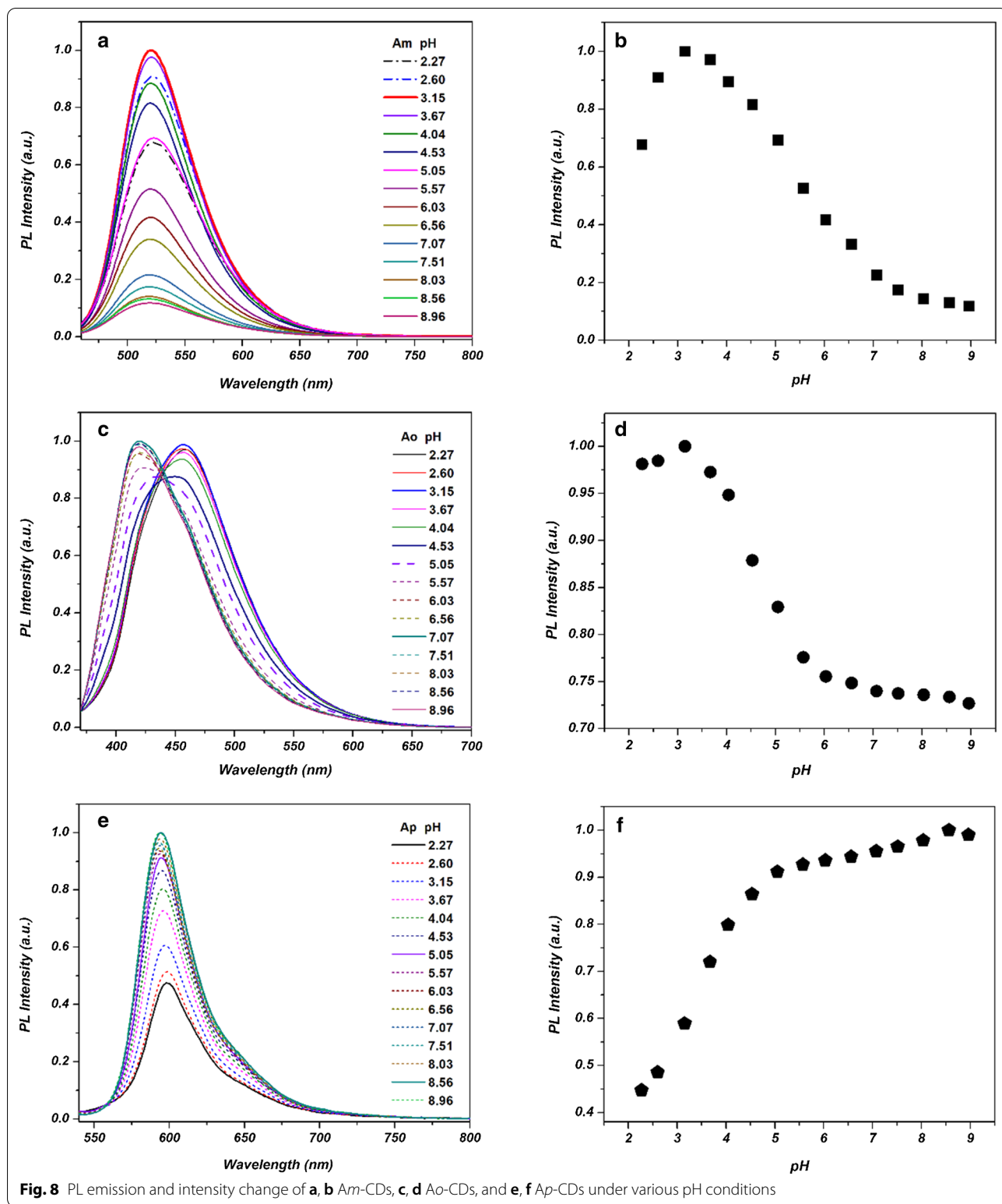
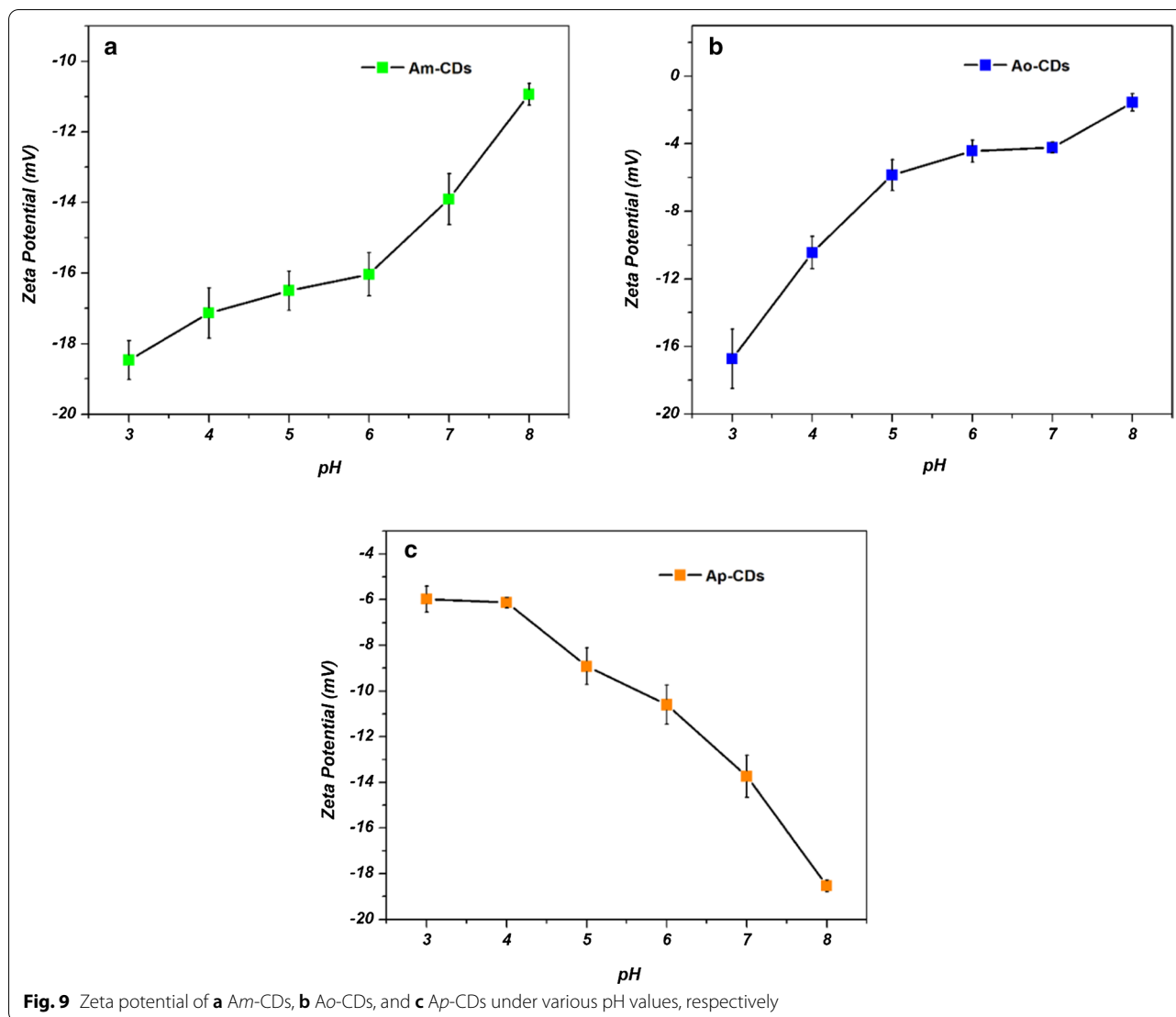


Fig. 8 PL emission and intensity change of **a, b** Am-CDs, **c, d** Ao-CDs, and **e, f** Ap-CDs under various pH conditions



increasing pH, whereas the zeta potential of Ap-CDs increased with increasing pH. This might result in lesser agglomeration and enhanced the PL intensity of Ap-CDs [30, 31].

Conclusion

In this work, the green, blue, and orange color emitting N-doped CDs have been successfully synthesized from the reaction between ascorbic acid (AA) and *m*-PDA, *o*-PDA, and *p*-PDA, respectively. For this purpose, a simple low temperature hydrothermal synthesis method has been employed. The photophysical and optical properties of the three CDs have been investigated thoroughly at different solvents and pH. The as-synthesized Ax-CDs exhibited higher QYs in ethanol than that in water. The lesser agglomeration, reduced rate of non-radiative decay, and lesser morphological change of CDs might

be the reason behind such behavior. In addition, the surface charge of synthesized Ax-CDs resulted in different pH-dependent PL emission properties. These unique properties of the as-synthesized CDs will enable their applications in different fields of imaging and sensing.

Supplementary information

Supplementary information accompanies this paper at <https://doi.org/10.1186/s11671-020-03453-3>.

Additional file 1. Supplementary Information.

Abbreviations

CDs: Carbon dots; AA: Ascorbic acid; *m*-PDA: *m*-Phenylenediamine; *o*-PDA: *o*-Phenylenediamine; *p*-PDA: *p*-Phenylenediamine; Ax-CDs: *x* = *m*, *o*, And *p*; QY: Quantum yield; SI: Supplementary Information; RT: Room temperature; QS: Quinine sulfate; PLE: Photoluminescence excitation; H₂O: Deionized water; MeOH: Methanol; EtOH: Ethanol; IPA: Isopropyl alcohol; ACE: Acetone;

ACN: Acetonitrile; DMF: *N,N*-Dimethylformamide; DMSO: Dimethyl sulfoxide; HR-TEM: High-resolution transmission electron microscopy; FT-IR: Fourier transform infrared spectroscopy; XRD: X-ray diffraction; XPS: X-ray photoelectron spectroscopy.

Acknowledgements

This study was supported by the Basic Science Research Program through the National Research Foundation of Korea (NRF) funded by The Ministry of Science, ICT and Future Planning (2019R1A2B5B02069683).

Authors' contributions

LW carried out the experiments and wrote this manuscript. JSC supported the analysis of all data. SHH guided all research steps and approved the final manuscript. All authors read and approved the final manuscript.

Funding

Basic Science Research Program through the National Research Foundation of Korea (NRF) funded by The Ministry of Science, ICT and Future Planning (2019R1A2B5B02069683).

Availability of data and materials

All data generated or analyzed during this study are included within this article and its supplementary information files.

Competing interests

The authors declare that they have no competing interests.

Received: 10 September 2020 Accepted: 24 November 2020

Published online: 03 December 2020

References

- Zhang J, Yu S-H (2016) Carbon dots: large-scale synthesis, sensing and bioimaging. *Mater Today* 19:382–393
- Atabaev TS (2018) Doped carbon dots for sensing and bioimaging applications: a minireview. *Nanomaterials* 8:342
- Lu D, Tang Y, Gao J, Wang Q (2018) Concentrated solar irradiation protocols for the efficient synthesis of tri-color emissive carbon dots and photophysical studies. *J Mater Chem C* 6:13013–13022
- Pal T, Mohiyuddin S, Packirisamy G (2018) Facile and green synthesis of multicolor fluorescence carbon dots from curcumin. *in vitro and in vivo bioimaging and other applications*. *ACS Omega* 3:831–843
- Wang C, Jiang K, Wu Q, Wu J, Zhang C (2016) Green synthesis of red-emitting carbon nanodots as a novel "turn-on" nanothermometer in living cells. *Chem A Eur J* 22:14475–14479
- Zhang J, Yuan Y, Liang G, Yu S (2015) Scale-up synthesis of fragrant nitrogen-doped carbon dots from bee pollens for bioimaging and catalysis. *Adv Sci* 2:1500002
- Qu Z-b, Zhou X, Gu L, Lan R, Sun D, Yu D, Shi G (2013) Boronic acid functionalized graphene quantum dots as a fluorescent probe for selective and sensitive glucose determination in microdialysate. *Chem Commun* 49:9830–9832
- Chen Y, Wu Y, Weng B, Wang B, Li C (2016) Facile synthesis of nitrogen and sulfur co-doped carbon dots and application for Fe(III) ions detection and cell imaging. *Sens Actuators B Chem* 223:689–696
- Jiang K, Sun S, Zhang L, Lu Y, Wu A, Cai C, Lin H (2015) Red, green, and blue luminescence by carbon dots: full-color emission tuning and multi-color cellular imaging. *Angew Chem Int Ed* 54:5360–5363
- Song L, Cui Y, Zhang C, Hu Z, Liu X (2016) Microwave-assisted facile synthesis of yellow fluorescent carbon dots from *o*-phenylenediamine for cell imaging and sensitive detection of Fe³⁺ and H₂O₂. *RSC Adv* 6:17704–17712
- Nie H, Li M, Li Q, Liang S, Tan Y, Sheng L, Shi W, Zhang SX-A (2014) Carbon dots with continuously tunable full-color emission and their application in ratiometric pH sensing. *Chem Mater* 26:3104–3112
- Qiao G, Lu D, Tang Y, Gao J, Wang Q (2019) Smart choice of carbon dots as a dual-mode onsite nanoplatfor for the trace level detection of Cr₂O₇²⁻. *Dyes Pigm* 163:102–110
- Ramanan V, Subray SH, Ramamurthy P (2018) A green synthesis of highly luminescent carbon dots from itaconic acid and their application as an efficient sensor for Fe³⁺ ions in aqueous medium. *New J Chem* 42:8933–8942
- Zhu S, Meng Q, Wang L, Zhang J, Song Y, Jin H, Zhang K, Sun H, Wang H, Yang B (2013) Highly photoluminescent carbon dots for multicolor patterning, sensors, and bioimaging. *Angew Chem Int Ed* 52:3953–3957
- Zhu J, Bai X, Bai J, Pan G, Zhu Y, Zhai Y, Shao H, Chen X, Dong B, Zhang H, Song H (2018) Emitting color tunable carbon dots by adjusting solvent towards light-emitting devices. *Nanotechnology* 29:085705
- Basiruddin S, Swain SK (2016) Phenylboronic acid functionalized reduced graphene oxide based fluorescence nano sensor for glucose sensing. *Mater Sci Eng C* 58:103–109
- Li L, Lu C, Li S, Liu S, Wang L, Cai W, Xu W, Yan X, Liu Y, Zhang R (2017) A high-yield and versatile method for the synthesis of carbon dots for bioimaging applications. *J Mater Chem B* 5:1935–1942
- Dang DK, Chandrasekaran S, Ngo Y-LT, Chung JS, Kim EJ, Hur SH (2018) One pot solid-state synthesis of highly fluorescent N and S co-doped carbon dots and its use as fluorescent probe for Ag⁺ detection in aqueous solution. *Sens Actuators B Chem* 255:3284–3291
- Jiao Y, Gong X, Han H, Gao Y, Lu W, Liu Y, Xian M, Shuang S, Dong C (2018) Facile synthesis of orange fluorescence carbon dots with excitation independent emission for pH sensing and cellular imaging. *Anal Chim Acta* 1042:125–132
- Khan S, Gupta A, Verma NC, Nandi CK (2015) Time-resolved emission reveals ensemble of emissive states as the origin of multicolor fluorescence in carbon dots. *Nano Lett* 15:8300–8305
- Khan WU, Wang D, Wang Y (2018) Highly green emissive nitrogen-doped carbon dots with excellent thermal stability for bioimaging and solid-state LED. *Inorg Chem* 57:15229–15239
- Pan L, Sun S, Zhang L, Jiang K, Lin H (2016) Near-infrared emissive carbon dots for two-photon fluorescence bioimaging. *Nanoscale* 8:17350–17356
- Chen J, Wei J-S, Zhang P, Niu X-Q, Zhao W, Zhu Z-Y, Ding H, Xiong H-M (2017) Red-emissive carbon dots for fingerprints detection by spray method: coffee ring effect and unquenched fluorescence in drying process. *ACS Appl Mater Interfaces* 9:18429–18433
- Wang H, Sun C, Chen X, Zhang Y, Colvin VL, Rice Q, Seo J, Feng S, Wang S, Yu WW (2017) Excitation wavelength independent visible color emission of carbon dots. *Nanoscale* 9:1909–1915
- Lee HJ, Jana J, Ngo Y-LT, Wang LL, Chung JS, Hur SH (2019) The effect of solvent polarity on emission properties of carbon dots and their uses in colorimetric sensors for water and humidity. *Mater Res Bull* 119:110564
- Wang L, Chung JS, Hur SH (2019) Nitrogen and boron-incorporated carbon dots for the sequential sensing of ferric ions and ascorbic acid sensitively and selectively. *Dyes Pigm* 171:107752
- Pan D, Zhang J, Li Z, Wu C, Yan X, Wu M (2010) Observation of pH-, solvent-, spin-, and excitation-dependent blue photoluminescence from carbon nanoparticles. *Chem Commun* 46:3681–3683
- Sun X, He J, Meng Y, Zhang L, Zhang S, Ma X, Dey S, Zhao J, Lei Y (2016) Microwave-assisted ultrafast and facile synthesis of fluorescent carbon nanoparticles from a single precursor: preparation, characterization and their application for the highly selective detection of explosive picric acid. *J Mater Chem A* 4:4161–4171
- Wang C, Xua Z, Cheng H, Lin H, Humphrey MG, Zhang C (2015) A hydrothermal route to water-stable luminescent carbon dots as nanosensors for pH and temperature. *Carbon* 82:87–95
- Sun Y, Wang X, Wang C, Tong D, Wu Q, Jiang K, Jiang Y, Wang C, Yang M (2018) Red emitting and highly stable carbon dots with dual response to pH values and ferric ions. *Microchim Acta* 185:83
- Guo Y, Wang Z, Shao H, Jiang X (2013) Hydrothermal synthesis of highly fluorescent carbon nanoparticles from sodium citrate and their use for the detection of mercury ions. *Carbon* 52:583–589

Publisher's Note

Springer Nature remains neutral with regard to jurisdictional claims in published maps and institutional affiliations.